

## MODEL ATMOSPHERES OF NEAR-EDDINGTON LIMIT X-RAY BURSTERS

ARIF BABUL AND BOHDAN PACZYŃSKI

Princeton University Observatory

Received 1986 December 12; accepted 1987 June 15

### ABSTRACT

We have developed some very simple, plane-parallel models of atmospheres of X-ray bursters that are very close to the Eddington limit. The dominant opacity source is assumed to be incoherent Thomson scattering. Free-free transitions are responsible for the creation of soft photons. At large optical depths,  $\tau > \tau_{bb}$ , we have LTE, while at small optical depths,  $\tau < \tau'$ , electron scattering is coherent. The bulk of the radiative flux at intermediate optical depths,  $\tau' < \tau < \tau_{bb}$ , is described by a Wien distribution with a chemical potential that varies with optical depth. We develop models with luminosities up to  $L = 0.9999L_E$ . At higher luminosities, it is necessary to allow for the sphericity of the extended, radiation pressure dominated atmospheres. The spectral (i.e. color) temperature in the extreme models is more than twice the effective temperature. Our spectra agree well with those calculated by London, Taam, and Howard, with a much more sophisticated computer program.

*Subject headings:* stars: atmospheres — stars: neutron — X-rays: bursts

### I. INTRODUCTION

In the past decade, considerable progress has been made toward understanding the phenomena of X-ray bursts (see reviews by Joss and Rappaport 1984 and Taam 1985). Type I X-ray bursts are thought to arise as a result of matter, accreted onto a neutron star surface, undergoing a thermonuclear flash. Numerical studies have shown that the thermonuclear flash model is quite successful at accounting for the global behavior of X-ray bursters; however, there are several remaining issues that need to be better understood.

One such problem is the relationship between the effective and the spectral temperatures of the X-ray bursters at burst maximum. Initially, neutron star atmospheres were assumed to be perfect blackbody emitters. However, van Paradijs (1982), Czerny and Sztajno (1983), London, Taam, and Howard (1984), and London *et al.* (1986) have suggested that the effects of electron scattering, both coherent and incoherent, in the neutron star atmosphere may be important enough to prevent the atmosphere from radiating as a perfect blackbody. London, Taam, and Howard (1984) and London *et al.* (1986), through detailed numerical analysis of the radiative transfer equations, investigated the effects of absorption, coherent electron scattering, as well as the effects of Comptonization on the X-ray spectra emitted by a neutron atmosphere. The results of their analysis reveal that the effects of electron scattering are indeed important; the scatterings deform the emitted X-ray spectrum from a Planck curve, resulting in a higher spectral temperature than the effective temperature. Ebisuzaki and Nomoto (1985), Madej (1986), and Lapidus, Sunyaev, and Titarchuk (1986) also arrived at similar conclusions. Foster, Ross, and Fabian (1986) present a detailed comparison between model atmospheres of neutron stars and the observed spectra of X-ray bursts.

In this paper, we present a very simple model of an atmosphere of a neutron star with the hope that the model will facilitate a better conceptual understanding of the effects of Comptonization, coherent scattering, and free-free processes

on the spectra when luminosity approaches the Eddington limit. The analysis of radiation transfer through our model atmosphere is quite tractable and may be done on any small computer. The flux spectra of X-rays emitted by our model atmosphere agree remarkably well with the spectra resulting from the detailed numerical simulations of London, Taam, and Howard (1984) and London *et al.* (1986) but with the advantage that the simplicity of our model allows us to study atmospheres with luminosities very close to the Eddington limit. In the next section, we discuss the basic assumptions, the input physics, and the relevant equations of our model and in § III, we discuss our findings, the limitations of our models, and the improvements that need to be incorporated into the model before a meaningful comparison between the theoretical and the observed spectra can be made.

### II. DEVELOPMENT OF MODEL

We consider a plane-parallel model atmosphere in hydrostatic and radiative equilibria, with luminosity close to the Eddington limit. Therefore, we assume that electron scattering is the dominant opacity source, with the free-free opacity being negligible at the frequencies where the radiation spectrum has its maximum. Following the conclusions by London *et al.* (1986) that the bound-free transitions are not important for X-ray bursts close to the Eddington limit, we have chosen to neglect these processes. The free-free transitions, on the other hand, are important as a source of new photons, but they do not affect the condition for hydrostatic equilibrium.

The equations of radiative and hydrostatic equilibria may be written as

$$\frac{dF}{dz} = 0, \quad (1a)$$

$$\frac{dP_g}{dz} = -g\rho \left(1 - \frac{F}{F_E}\right), \quad (1b)$$

where

$$F = \int_0^\infty F_\nu d\nu = \frac{L}{4\pi R^2} = \text{constant}, \quad (2a)$$

$$F_E = \frac{gc}{\kappa_{es}} = \text{constant}, \quad (2b)$$

$$P_g = \frac{k_B}{\mu m_H} \rho(\tau) T_e(\tau), \quad d\tau = -\rho \kappa_{es} dz; \quad (2c)$$

$T_e$  is the electron temperature, which is equal to the ion temperature,  $g$  is the gravitational acceleration at the neutron star surface,  $\kappa_{es}$  is the electron scattering opacity, and  $\tau$  is the corresponding electron scattering optical depth. Equation (1b) can be integrated to obtain the density stratification of the atmosphere as a function of optical depth, provided that the electron temperature is known:

$$P_g(\tau) = \frac{g}{\kappa_{es}} \left(1 - \frac{F}{F_E}\right) \tau, \quad (3)$$

$$\rho(\tau) = \frac{\mu m_H g}{k_B \kappa_{es}} \left(1 - \frac{F}{F_E}\right) \frac{\tau}{T_e(\tau)}.$$

It is very important that within our approximation  $\kappa_{es}$  is a constant, independent of photon frequency or electron temperature. In this case, the mean radiation intensity,  $J$ , is a function of the optical depth  $\tau$ ,

$$J(\tau) = \frac{3}{4} F[\tau + q(\tau)], \quad (4)$$

where  $q(\tau)$  is the Hopf function [see Kourganoff 1963, p. 99 for numerical approximations to  $q(\tau)$ ]. For our purpose, we adopt the Eddington approximation, i.e.,  $q(\tau) = \frac{2}{3}$ .

We assume that at a large optical depth, the atmosphere is in LTE; therefore, the radiation has a Planck distribution with temperature equal to the local electron temperature:

$$J(\tau) = B(T_e) = \frac{\sigma}{\pi} T_e^4(\tau), \quad \tau \geq \tau_{bb}. \quad (5)$$

It may be shown (see Paczyński and Anderson 1986) that at this large optical depth, we have

$$1 - \beta \equiv \frac{P_{\text{rad}}}{P} = \frac{F}{F_E}, \quad (6)$$

and  $\beta$  is a very convenient parameter to use to describe the models. At smaller optical depths, LTE cannot be assumed, and we have to find the distribution of electron temperature with optical depth.

For a neutron star with a given mass, radius, and therefore, a given surface gravity  $g$ , the radiation flux may vary almost all the way up to the Eddington limit. However, as the radiative flux increases, the radiation pressure becomes dominant, and the density scale height in the atmosphere increases. The density scale height is defined as

$$h_\rho \equiv \left| \frac{d \ln \rho}{dz} \right|^{-1}. \quad (7)$$

By the time  $\beta$  is down to  $10^{-4}$ , the scale height is about equal to the neutron star radius,

$$\frac{h_\rho}{R} \approx \frac{k_B T_e}{\mu M_H GM/R} \frac{1}{\beta} \approx 1, \quad (8)$$

and the atmosphere becomes spherically symmetric (Paczyński and Anderson 1986). This lower limit,  $\beta \approx 10^{-4}$ , is also the necessary and sufficient condition for the expansion of the photospheric radius during an X-ray burst. Therefore, we shall consider only models with  $\beta \geq 10^{-4}$ .

Since we are interested in atmospheres that are dominated by electron scattering, it is convenient to divide the atmosphere into a total of six regions in the electron scattering optical depth–photon energy plane (see Fig. 1). At large optical depths,  $\tau > \tau_{bb}$  (region III), we assume LTE. New photons are created due to free-free transitions at low frequencies, and incoherent electron scattering redistributes them in frequency, maintaining a Planck distribution. At  $\tau < \tau_{bb}$ , the rate at which the photons diffuse out toward the surface is higher than the rate

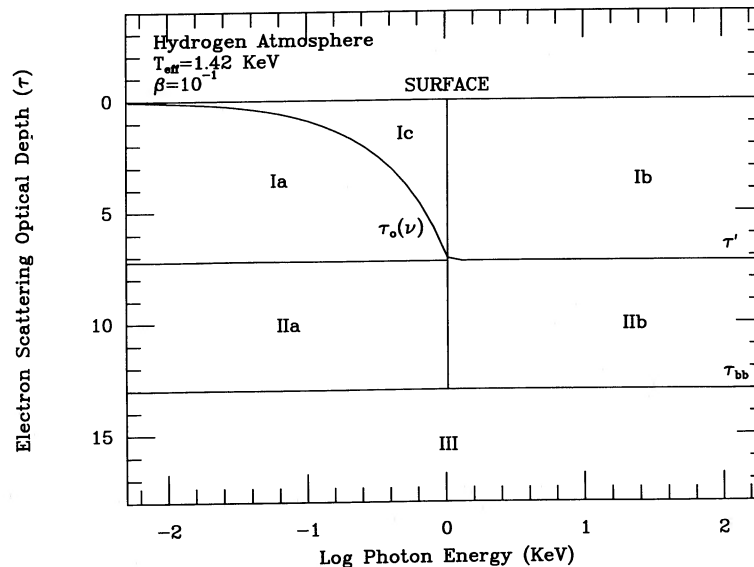


FIG. 1.—Division of a model atmosphere into distinct regions in the electron scattering optical depth–photon energy plane for the purpose of approximating the emitted X-ray spectrum.

at which they may be created by free-free processes. Therefore, LTE cannot be maintained. At low frequencies, free-free processes force the radiation to maintain a Planck distribution at the local electron temperature (regions Ia and IIa); however, most of the radiation is at high frequencies (region Ib and IIB) where there is a deficiency in the photon number density as the photons escape to the surface faster than they are up-scattered from the free-free dominated frequencies. We assume that in regions Ib and IIB, no new photons are created; we also assume that practically all the radiative flux is carried at these high frequencies. The division into regions Ib and IIB is due to the difference in the efficiency of Comptonization. We assume that Comptonization is fully efficient at moderate optical depths,  $\tau' < \tau < \tau_{bb}$  (region IIB), and that there is no Comptonization at small optical depths,  $\tau < \tau'$  (region Ib). In other words, we assume that in region IIB, the total radiative flux is conserved while in region Ib, we have monochromatic flux conservation. Full Comptonization in region IIB means that we have a Bose-Einstein spectrum there, with an integrated intensity  $J(\tau)$  characterized by the local electron temperature and a nonzero chemical potential. To allow for a semianalytic treatment of the model, we approximated the Bose-Einstein distribution by a Wien distribution.

At low frequencies, it is convenient to define a "true" photosphere, located at  $t_0(\nu)$ , as the electron scattering optical depth at which the soft photons emerging from the surface are typically created. In the very low frequency region, where free-free opacity dominates over electron scattering opacity, the "true" photosphere is near the surface of the atmosphere, at electron scattering optical depth  $\tau_0(\nu) \approx 0$ . For very low frequencies, the value of the optical depth due to free-free opacity at the photosphere is  $\tau_{ff}(\nu) \approx 1$ . At somewhat higher frequencies, the "true" photosphere is a little deeper, as shown in Figure 1. Above the "true" photosphere (region Ic), almost no photons are created, and incoherent scattering is not important. Therefore, we have monochromatic conservation of radiative flux, as in region Ib.

It should be clear from our description that there is no direct coupling between regions Ia and IIa, where the soft photons are created, and the high-frequency regions, Ib and IIB. There-

fore, one may wonder whether the low-frequency regions are of any importance. The low-frequency regions are indeed important since they affect the electron temperature at small and medium optical depths, which in turn affects the Comptonization of high-energy photons. At each optical depth, the electron temperature is determined by a balance between the heating of electrons due to high-frequency photons, and the cooling of electrons by low-frequency photons and the free-free processes. A full-scale model should calculate this energy balance in a self-consistent way at all optical depths. We shall calculate this balance at  $\tau = \frac{2}{3}$  only, and we shall assume that  $T_e^4$  is a linear function of optical depth between the surface and  $\tau_{bb}$ , where LTE is maintained. In order to calculate the radiation field, we need to know the electron temperature as a function of optical depth. Hence, we proceed in the following manner.

For a model with a given chemical composition, effective temperature, and  $\beta$ , we took the electron temperature at  $\tau = \frac{2}{3}$  to be an adjustable parameter. We calculated the radiation field for various values of this parameter and then determined the value of the electron temperature at  $\tau = \frac{2}{3}$  that followed from the radiation field. For every model, there was only one value of  $T_e(\frac{2}{3})$  that turned out to be consistent with the calculated radiation field. Figure 2 shows the spectrum of flux emitted by the atmosphere described in Figure 1. The flux curve is marked so as to show the regions of its origin.

In order to determine, quantitatively, the spectrum of the radiation emitted by a neutron star atmosphere, we divided the atmosphere into two regions:  $\tau \leq \tau'$  and  $\tau \geq \tau'$ , where

$$\tau'^2 = \left[ \frac{m_e c^2}{4k_B T_e(\tau')} \right] \quad (9)$$

corresponds to the number of scatterings required to Comptonize the low-frequency photons (Rybicki and Lightman 1979). Following Felton and Rees (1972), we claim that the emergent radiation may be regarded, in a first-order approximation, as a sum of two components: a nonthermalized bremsstrahlung continuum emerging from the "skin" of thick-

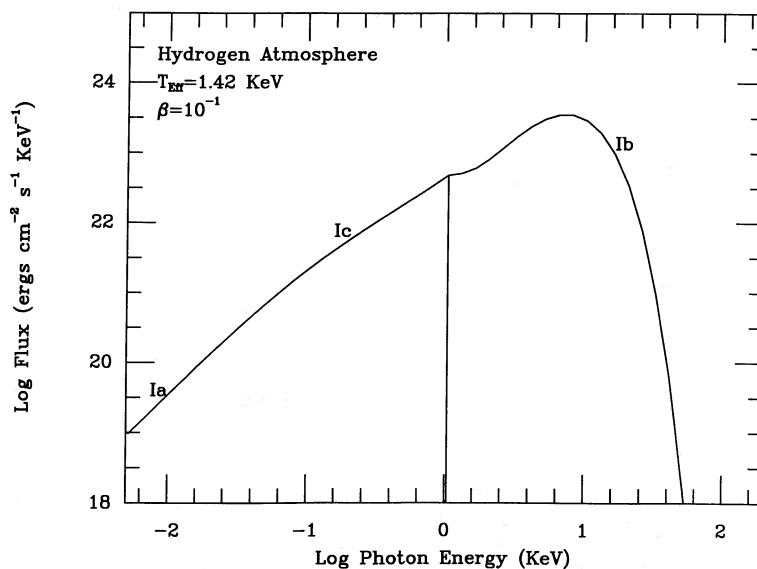


FIG. 2.—Spectrum of X-ray radiation emitted by the model atmosphere of Fig. 1. Vertical line delineates the boundary between the low- and the high-frequency regions of the spectrum. Flux curve is marked so as to show the regions of its origin in Fig. 1.

ness  $\tau'$  just as if the source were a definite slab of this thickness, and a thermalized equilibrium distribution emerging from the deeper layers.

The radiation emerging from the slab of thickness  $\tau'$  was calculated by generalizing the method of Felton and Rees (1972). In a homogeneous, isothermal, semi-infinite medium, the maximum depth from which a photon of given frequency can escape without being absorbed is given by

$$[\tau_{\text{ff}}(\nu) + \tau]\tau_{\text{ff}} \approx 1, \quad (10)$$

where

$$d\tau_{\text{ff}} = -\rho(\tau)\kappa_{\text{ff}}(\nu)dz, \quad (11a)$$

$$\kappa_{\text{ff}}(\nu) = \frac{3.7 \times 10^8}{\sqrt{T_e(\tau)}} \nu^{-3} \frac{Z^2 \rho}{\mu_i \mu_e m_H^2} [1 - e^{-h\nu/k_B T_e(\tau)}] \bar{g}_{\text{ff}}, \quad (11b)$$

$$\bar{g}_{\text{ff}} = \begin{cases} \frac{\sqrt{3}}{\pi} \ln \left( 2.2 \frac{k_B T_e(\tau)}{h\nu} \right), & \frac{h\nu}{k_B T_e} \leq 1, \\ \frac{\sqrt{3}}{\pi} \ln \left( 2.2 \sqrt{\frac{k_B T_e(\tau)}{h\nu}} \right), & \frac{h\nu}{k_B T_e} \geq 1. \end{cases} \quad (11c)$$

In the above equations,  $\kappa_{\text{ff}}(\nu)$  is the free-free absorption opacity,  $\tau_{\text{ff}}$  is the corresponding optical depth,  $Z$  is the charge of the ions,  $\bar{g}_{\text{ff}}$  is the velocity averaged Gaunt factor (Lightman 1981), and all other symbols have their usual meaning.

For an atmosphere with temperature gradient and density stratification, eq. (10) is not valid. Felton and Rees (1972) attempted to calculate the critical depth at which the radiation field will approach blackbody (see eqs. [56] and [57] in their paper) for atmospheres with the above-mentioned structure; however, their equations are valid only for high-frequency photons where  $\tau_{\text{ff}}(\nu) \ll \tau$  and, therefore, need to be generalized in order to treat photons of all frequencies. We claim that for a photon traveling toward the surface, the probability of absorption at an electron scattering optical depth  $\tau$ ,

$$dA \approx 2[\tau_{\text{ff}}(\tau) + \tau] \frac{d\tau_{\text{ff}}}{d\tau} d\tau. \quad (12a)$$

For low-frequency photons,  $\tau_{\text{ff}}(\nu) \gg \tau$ , and scattering of photons by electrons can be neglected. In this regime, the above equation suggests that the probability of absorption is  $dA \approx 2\tau_{\text{ff}} d\tau_{\text{ff}}$ , and that the photons of a given frequency, which escape from the surface, are emitted at an optical depth,  $\tau_0$ , such that  $\tau_{\text{ff}}(\tau_0) \approx 1$ . For high-frequency photons,  $\tau_{\text{ff}}(\nu) \ll \tau$ , and we recover Felton and Rees' eq. (56). Therefore, in general, the maximum depth,  $\tau_0(\nu)$ , from which a photon of given frequency can escape, is given by the condition:

$$\int_0^{\tau_0(\nu)} 2[\tau_{\text{ff}}(\tau) + \tau] \frac{d\tau_{\text{ff}}}{d\tau} d\tau \approx 1. \quad (12b)$$

In Figure 1, we have plotted  $\tau_0(\nu)$  versus photon energy for the "skin" layer.

At the low-frequency end,  $\tau_0(\nu)$  is very small. Thus, the escaping radiation comes from the layers near the surface and is not affected by electron scattering, giving rise to a "self-absorbed" spectrum. At intermediate frequencies, photons from deeper inside the "skin" layer also begin to contribute to the emergent flux. Hence, the flux begins to deviate from a "self-absorbed" spectrum as these photons are affected by coherent scattering. At some frequency,  $\tau_0(\nu)$  equals  $\tau'$  and for higher frequencies, the depth from which photons can escape,

exceeds the thickness of the "skin" layer. However, since the photons emitted from the layers deeper than  $\tau'$  undergo sufficient number of incoherent scatterings to redistribute them into a thermalized distribution, we assert that these photons are accounted for by the second of the two components of the emergent radiation and, therefore, need not be considered when calculating the nonthermalized bremsstrahlung component of the escaping flux. Hence, for frequencies such that  $\tau_0(\nu)$  exceeds  $\tau'$ , only the photons created within the "skin" layer need to be considered. The component of emergent flux due to the "skin" layer is given by

$$F_{\nu, \text{low}} \approx \int_0^{\min[\tau', \tau_0(\nu)]} \pi B_\nu(\tau) \frac{d\tau_{\text{ff}}}{d\tau} d\tau. \quad (13)$$

The second component of the emergent flux is the thermalized equilibrium distribution coming from layers deeper than  $\tau'$ . This component dominates the high-frequency end of the emergent flux. At depths  $\tau \geq \tau'$ , the temperature of the distribution is equal to that of the surrounding electrons. Of the processes that force the photon distribution to thermalize, the dominant mechanism is Comptonization of low-frequency photons. However, as previously discussed, this mechanism is relatively ineffective for  $\tau < \tau'$ , and, therefore, although this thermalized radiation will heat the electrons in the "skin" layer as it traverses through, its characteristic temperature will not change appreciably. Hence, we assume that the spectral distribution of the thermalized radiation is the same as that at  $\tau = \tau'$ , attenuated due to coherent electron scatterings. We approximate the effects of coherent electron scattering by applying the Eddington approximation in the monochromatic limit. Therefore,

$$F_{\nu, \text{high}} \approx \frac{2\pi J_\nu(\tau')}{[1 + (3/2)\tau']}, \quad (14a)$$

$$J_\nu(\tau') \approx \frac{2h\nu^3}{c^2} e^{-\mu(\tau')} e^{-h\nu/k_B T_e(\tau')}, \quad (14b)$$

where  $\mu(\tau)$ , the chemical potential of the photon distribution, is the measure of the deficiency in the photon number density as compared to the blackbody number density ( $\mu = 0$ ).

Hence, the total emergent flux spectrum is given by

$$F_\nu = F_{\nu, \text{low}} + F_{\nu, \text{high}}. \quad (15)$$

Assuming that  $\int F_{\nu, \text{high}} d\nu \gg \int F_{\nu, \text{low}} d\nu$ , the total integrated flux is given by

$$F \approx \frac{24\pi}{c^2 h^3} e^{-\mu(\tau')} \frac{[k_B T_e(\tau')]^4}{1 + (3/2)\tau'}. \quad (16)$$

We would expect the total integrated flux to be equal to  $\sigma T_{\text{eff}}^4$ ; however, since we used the Wien approximation (eq. [14b]) to calculate the integrated flux, we incurred a maximum error of 8% (Fu and Arnett 1986). To avoid this error, we compare equation 16 not to  $\sigma T_{\text{eff}}^4$  but to

$$F = \int_0^\infty \frac{2\pi h\nu^3}{c^2} e^{-h\nu/k_B T_{\text{eff}}} = \frac{12\pi}{c^2 h^3} (k_B T_{\text{eff}})^4, \quad (17)$$

yielding

$$\mu(\tau') = 4 \ln \left[ \frac{T_e(\tau')}{T_{\text{eff}}(\tau')} \right], \quad (18)$$

where  $T_E(\tau)$  is the Eddington temperature:

$$T_E^4(\tau) \equiv \frac{1}{2} T_{\text{eff}}^4 (1 + \frac{3}{2} \tau). \quad (19)$$

It can be seen from equation (18) that as  $T_e(\tau)$  approaches  $T_E(\tau)$  deep inside the atmosphere,  $\mu(\tau)$  vanishes and the mean spectral intensity (eq. [14b]) approaches the blackbody Wien distribution, as would be expected.

To complete the model, the temperature profile of the atmosphere needs to be defined. Under our scheme, there are two possible temperature profiles, depending on the relative values of  $\tau'$  and  $\tau_{\text{bb}}$ . The latter is the optical depth at which the escape time for high-frequency photons ( $\nu \geq \nu_*$ ) is equal to the time it takes to produce a blackbody photon number density by bremsstrahlung (Lightman 1981). This optical depth is given by

$$\tau_{\text{bb}}^{3/2} \approx \frac{1.0884 \times 10^{-9}}{\bar{g}_{\text{ff}}(\nu_*)} T_E^{9/4}(\tau_{\text{bb}}) \sqrt{\frac{1}{\mu \mu_e} \frac{1}{Z^2} \frac{1}{g \beta}}, \quad (20)$$

where the surface gravity,  $g$ , in terms of the parameters of our model, is

$$g = \frac{\kappa_{\text{es}} \sigma T_{\text{eff}}^4}{c (1 - \beta)}. \quad (21)$$

and  $\nu_*$  is such that

$$\tau_{\text{bb}} = \left[ \frac{m_e c^2}{4 k_B T_E(\tau_{\text{bb}})} \right] \tau_{\text{ff}}(\nu_*, \tau_{\text{bb}}). \quad (22)$$

We shall only discuss the case,  $\tau_{\text{bb}} > \tau'$ , the case associated with our models. For  $\tau \geq \tau_{\text{bb}}$ , we claim that both the electron and the radiation temperatures are equal and can be approximated by the Eddington temperature profile (eq. [19]), a linear relationship in the  $T^4$  versus  $\tau$  plane. For  $\tau \leq \tau_{\text{bb}}$ , Compton effects will cause the temperature structure to deviate from that of LTE. For simplicity, we chose to approximate this deviation with another linear relationship in the above plane. Therefore, the profiles of the electron temperature and of the temperature characterizing the photons in the Wien distribution (radiation temperature), for  $\tau \leq \tau_{\text{bb}}$ , are of the form:

$$\begin{aligned} T_e^4(\tau) &= A(\tau - \tau_{\text{bb}}) + T_E^4(\tau_{\text{bb}}), & \tau \geq \tau_{\text{bb}}, \\ T_{\text{rad}}(\tau) &= \begin{cases} T_e(\tau) & \tau' \leq \tau \leq \tau_{\text{bb}} \\ T_e(\tau') & \tau \leq \tau' \end{cases}, & \tau \leq \tau' \end{aligned} \quad (23)$$

In order to solve for the unknown constant,  $A$ , we required the electron temperature to satisfy the following condition:

$$\left. \frac{dE_C}{dt} \right|_{\tau=2/3} + \left. \frac{dE_{\text{ff}}}{dt} \right|_{\tau=2/3} = 0, \quad (24)$$

that is, at the photosphere, there exists an equilibrium between the heating of electrons by the hot photons in the thermalized distribution and the cooling of electrons by free-free processes. The rate of energy transfer from the electrons to the photons, due to Comptonization, is given by Pozdnyakov, Sobol', and Sunyaev (1983) to be

$$\frac{dE_C}{dt} = \frac{\sigma_T}{m_e c^2} \frac{4\pi\rho}{\mu_e m_H} \int_0^\infty \left( 4k_B T_e J_\nu - h\nu J_\nu - \frac{1}{2} \frac{c^2}{\nu^2} J_\nu^2 \right) d\nu. \quad (25)$$

This is the integrated form of Kompaneets equation (Kompaneets 1957). The loss of energy from the electrons, due

to bremsstrahlung emission, is

$$\frac{dE_{\text{ff}}}{dt} = 4\pi\rho \int_0^\infty \kappa_{\text{ff}}(\nu) [B_\nu(T_e) - J_\nu] d\nu. \quad (26)$$

We approximated  $J_\nu(\tau = \frac{2}{3})$  to be twice the mean monochromatic intensity of radiation at the surface.

### III. DISCUSSION

In order to test our model, we sought to compare the predicted flux spectrum with that acquired by London *et al.* (1986). We chose their only single-component atmosphere, a helium atmosphere with parameters:  $T_{\text{eff}} = 2.84$  keV and  $\beta = 0.565$  ( $\log g = 15$ ), as a standard. It should be noted that our model is not at its best at such large values of the  $\beta$  parameter since our approximation that regions Ia, Ib, and Ic (see Fig. 1) are well-separated and can be treated discontinuously works best when electron scattering is dominant, and this occurs when the luminosity is close to the Eddington limit ( $\beta \ll 1$ ). Nevertheless, our flux spectrum agreed remarkably well with the standard mentioned above. The two flux spectra are presented, for comparison, in Figure 3.

In Figures 4–7, we present flux curves with  $\beta$  fixed at an extreme value of  $10^{-4}$  but with different effective temperatures and with atmospheres of different chemical compositions. On each graph, we have also plotted a blackbody curve corresponding to the effective temperature and a normalized blackbody curve fitted to the peak of the spectrum. We term the temperature of the latter blackbody curve “the spectral temperature.” In some of the figures, at the low-frequency end, the flux curve crosses over the blackbody curve corresponding to the effective temperature. The crossover implies that the temperature close to the surface may be higher than the effective temperature, as would be expected if the heating of the electrons by radiation strongly counters the cooling effect of bremsstrahlung emission. It should be noted that since only radiation near the peak of the X-ray spectrum can be directly observed and that nothing is known about the spectrum of X-ray bursters below photon energy of 1 keV, the low-energy portion of the flux curves presented in Figures 4–7 is of little importance with respect to the observations.

We investigated 22 model atmospheres resulting from various combinations of four values of  $\beta$  ( $10^{-4}$ ,  $10^{-3}$ ,  $10^{-2}$ ,  $10^{-1}$ ), two values of the effective temperature (1.42 keV and 2.84 keV), and three different types of atmospheres (nickel, helium, hydrogen). We found that the spectral hardening factor  $T_{\text{spec}}/T_{\text{eff}}$ , varied from 1.6 to 2.6. The factor increased as  $\beta$  was decreased, increased as the charge of the ions in the atmosphere was decreased, and also increased as the effective temperature was decreased.

To understand the first two effects, we show, in Figure 8, the variations in the flux spectra due to the variations in the  $\beta$  parameter in a helium atmosphere. This variation can be easily understood if it is noted that as  $T_{\text{eff}}$  remains constant, an increase in  $\beta$  (or a decrease in the luminosity) actually implies an increase in the density of the atmosphere, and, since a dense atmosphere emits more bremsstrahlung radiation, its surface is cooler than that of a less dense atmosphere. Furthermore, a higher bremsstrahlung emission rate also implies that the depth at which the spectrum becomes blackbody is closer to the surface, and, therefore, the Wien peak is cooler and has a very small chemical potential.

The variation in the  $T_{\text{spec}}/T_{\text{eff}}$  due to the chemical composi-

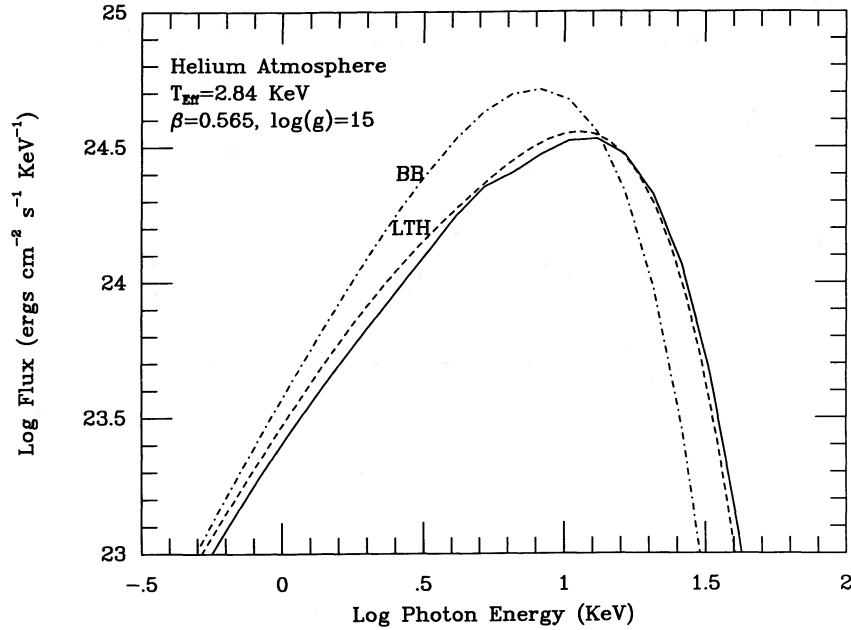


FIG. 3.—Comparison of the emergent flux from our model atmosphere (solid curve), with the spectrum determined by London *et al.* (1986) (dashed curve “LTH”) for atmosphere with same parameters. Dot-dashed curve (“BB”) is the Planck function evaluated at the effective temperature of the atmosphere.

tion of the model atmosphere can also be understood in similar terms. The strength of the free-free processes depends not only on the density, as discussed above, but also on  $Z^2$ , where  $Z$  is the charge of the ions in the atmosphere. Therefore, a high- $Z$  model has a larger bremsstrahlung component and acts very much like the high- $\beta$  model described above. Hence, the same reasoning used in the case of varying  $\beta$  parameter (or the luminosity) may be used to explain the variations in the flux curves and the variations in the spectral hardening factor due to changes in the atmosphere’s chemical composition. Figure 9

shows the flux spectra of atmospheres of differing chemical composition.

We also found that for  $\tau \leq \tau_{bb}$ , our model atmospheres tended toward developing an isothermal structure, with the effect being more pronounced for models with low  $Z$ , low  $\beta$ . As discussed above, such models do not have large bremsstrahlung emission rates; therefore, Compton heating/cooling manages to establish a nearly isothermal temperature profile. Assuming that  $\beta \sim 10^{-7}$  and that the atmosphere is isothermal above  $t_{bb}$ , London *et al.* (1986) arrived at an analytic expres-

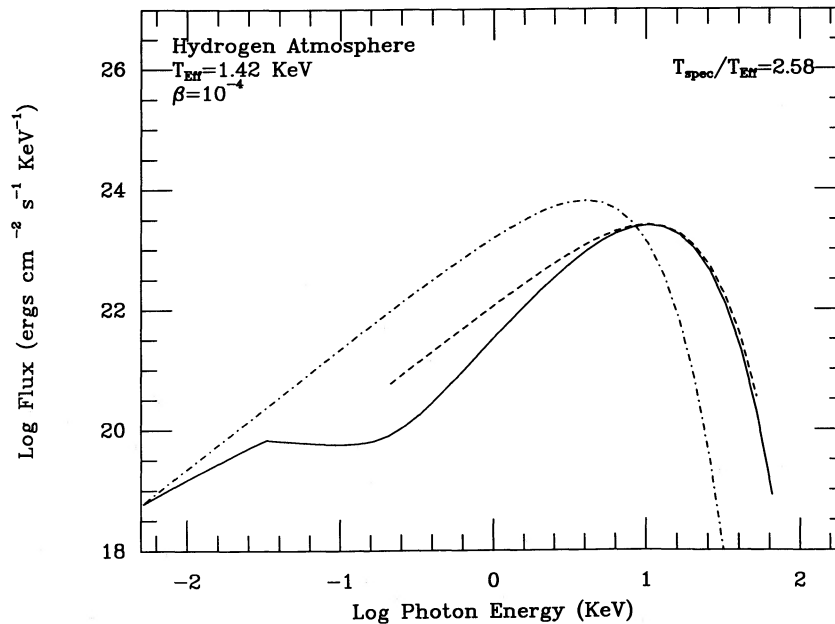


FIG. 4.—Solid curve is the spectrum of emitted flux from atmosphere of model 1. Dashed curve is the normalized Planck curve that best fits the peak of the spectrum. Spectral temperature is defined as the temperature characterizing this Planck curve. Dot-dashed curve corresponds to the Planck curve evaluated at the effective temperature of the atmosphere.

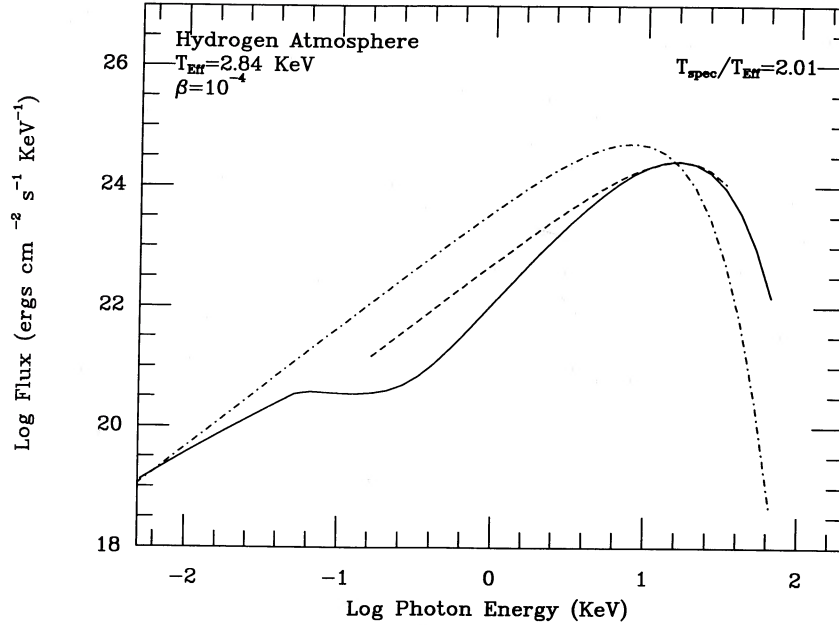


FIG. 5.—Same as Fig. 4, for model 5

sion for the spectral hardening factor  $T_{\text{spec}}/T_{\text{eff}}$ . Comparing the analytic results to our calculated values for models 1 and 5, we found that the analytic results were greater by a factor of  $\sim 1.5$ .

London *et al.* (1986) also found that the dependence of  $T_{\text{spec}}/T_{\text{eff}}$  upon the effective temperature is rather complicated due to many feedbacks in the system. In light of this, we do not feel qualified to discuss the effects of  $T_{\text{eff}}$  upon the spectral hardening factor for our flux curves since we have considered only two values for the effective temperature. We refer interested readers to the paper mentioned above for a more detailed discussion on this topic.

We believe that our models are as simple as possible while retaining the most important physical processes responsible for

the formation of the spectra from electron scattering atmospheres of X-ray bursters. We would like to emphasize that we did not encounter any numerical problems with our approach, even in models with  $L/L_E = 0.9999$ , although our models are not good for  $L/L_E < 0.1$ . However, there are some serious limitations.

For simplicity, we assumed that the electron scattering cross section does not depend on the photon energy; i.e., we worked in the Thompson limit. This seems reasonable since we have  $k_B T \ll m_e c^2$ . However, the gas density, as calculated with equation 3, is proportional to  $(1 - F/F_E)$ , and, of course,  $F_E$  is inversely proportional to  $\kappa_{\text{es}}$ , as given by equation (2b). Since the total radiation flux,  $F$ , is constant, and in some of our

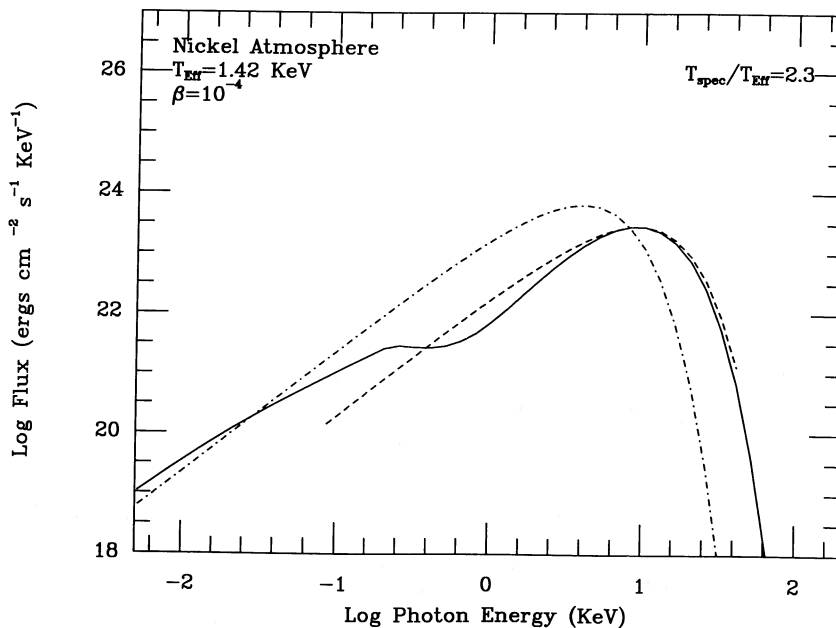


FIG. 6.—Same as Fig. 4, for model 17

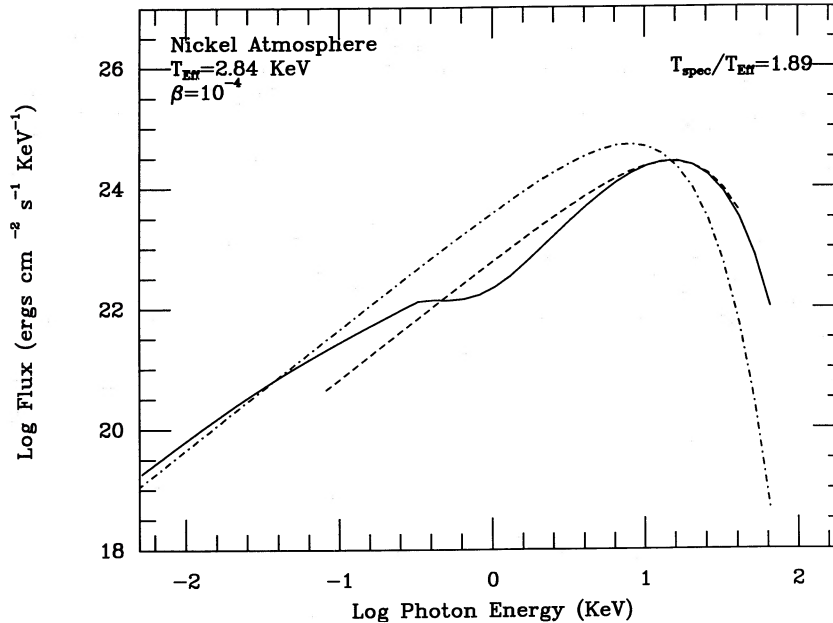
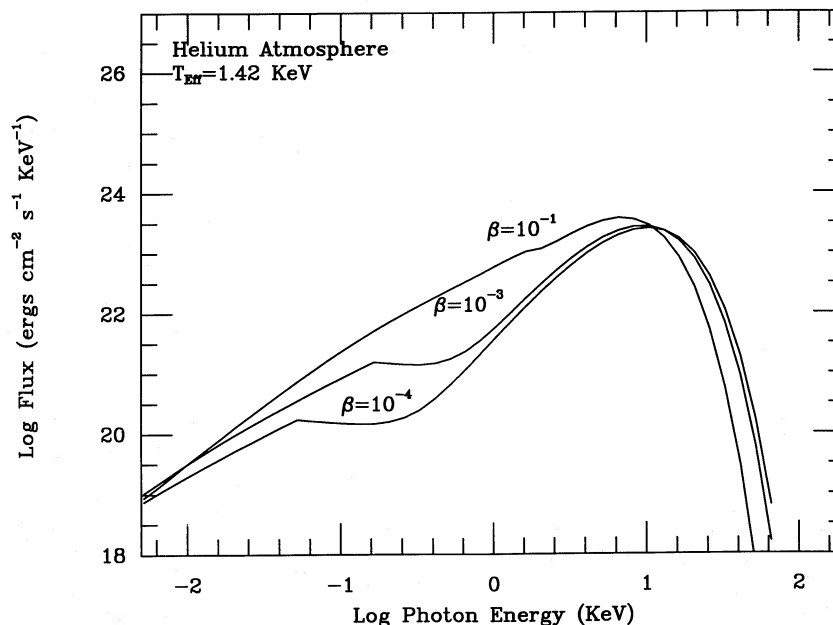


FIG. 7.—Same as Fig. 4, for model 20

models  $F = 0.9999F_E$ , it is clear that even a very small reduction of the mean value of the electron scattering opacity with optical depth will result in a very large increase in the gas density and in the strength of the free-free emission. In fact, the expected variation in  $\kappa_{es}$ , in the atmosphere, is not all that small, since our models reach LTE at a rather large optical depth,  $\tau_{bb}$  (see Table 1), where the temperature may be up to 3 times higher than it is at the surface. We conclude that by adopting the Thompson scattering cross section, we underestimate the importance of free-free emission and we overestimate the difference between the effective and spectral temperatures. Our error increases as the luminosity approaches the Eddington limit.

In treating the high-frequency component of the radiation, we chose to approximate the photon distribution by a Wien distribution instead of using a Bose-Einstein distribution with a nonzero chemical potential. Using the exact B-E distribution, instead of the Wien approximation, would not lead to a significant change in the emergent X-ray spectrum. However, when considering the energy balance between the photons and the electrons, the Wien approximation affects the equilibrium electron temperature at the photosphere, thereby affecting the temperature profile throughout the atmosphere. In particular, due to the presence of the term associated with induced heating of electrons in the integrated form of Kompaneets equation (the third term on the right side of eq. [25]), the use of a Wien

FIG. 8.—Flux distributions for the atmospheres of models 9, 10, and 12. Curves reveal the effect of  $\beta$  parameter on the distribution.

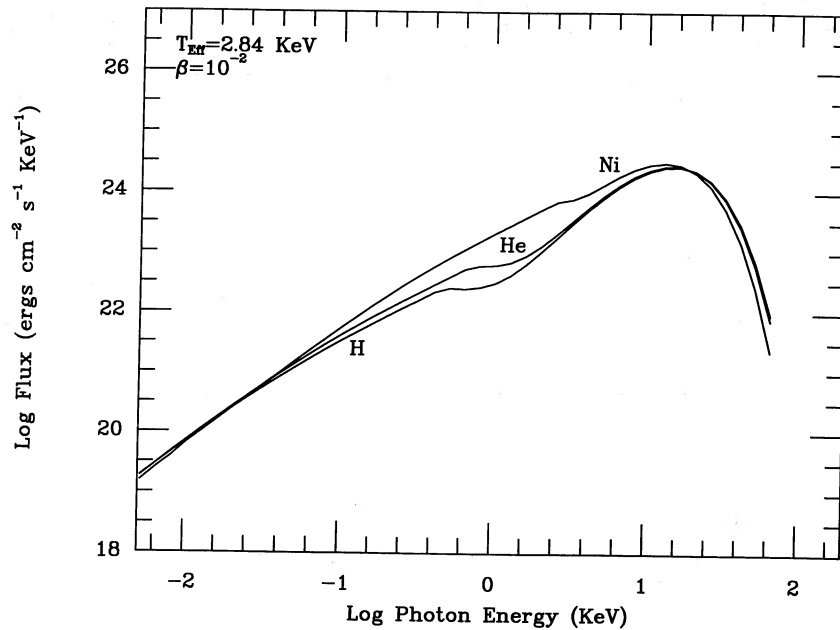


FIG. 9.—Emergent flux from atmospheres of models 7, 15, and 22. Curves show the effect, on the spectrum, of the chemical composition of the atmosphere.

distribution, instead of a Bose-Einstein spectrum, in this equation leads to an overestimation of the heating of the electrons and, therefore, an overestimation of the electron temperature, at the photosphere. We expect the excess heating to increase in magnitude as the luminosity approaches the Eddington limit.

The *ad hoc* manner of calculating the spectrum across the transition region between the low- and the high-frequency components is also a cause for concern. The electron heating

and cooling rates depend very strongly upon the shape of the flux curve across the transition region. Therefore, a better method for estimating the flux across the transition region needs to be developed.

Furthermore, as our model does not allow for the calculation of the electron and the Wien temperature at all optical depths, we are required to specify the temperature profile in the atmosphere, introducing a degree of arbitrariness in the model. As discussed earlier, our choice for the temperature distribution above  $\tau_{bb}$  was motivated by the desire to model the deviation from LTE in as simple a manner as possible. In order to determine fully the atmosphere's temperature structure, we only need to consider the energy balance at the photosphere. However, we pay a price for opting for simplicity. The temperature structure in our model atmospheres is rather sensitive to variations in the heating/cooling rates at the photosphere. Any change in the photospheric temperature, whether due to increased bremsstrahlung resulting from a correct treatment of the electron scattering opacity or due to changes in the bremsstrahlung and Compton heating/cooling rates resulting from a more exact treatment of the high-frequency component of the radiation as well as a better treatment of the transition region between the high- and low-frequency components, would exert a "long lever arm" on the whole atmospheric structure down to  $\tau_{bb}$  (London, private communication). In order to alleviate the atmosphere's sensitivity to the value of the photospheric temperature, a simple method for estimating the equilibrium temperature at all optical depths needs to be developed.

We also assumed that for  $\tau \leq \tau'$ , the Wien peak is affected only by coherent scattering; however, the very hot photons in the high-energy tail ( $h\nu > k_B T_e$ ) continue to interact until  $\tau \sim m_e c^2 / k_B T_{rad}$  (Sunyaev and Titarchuk 1980), causing a slight steepening of the emergent flux curve at very high frequencies.

Finally, there are other physical phenomena, which are much more difficult to treat and which also need to be taken into account at the same time: sphericity of the atmospheres and general relativity. Paczyński and Anderson (1986) showed

TABLE 1  
PARAMETERS OF MODEL ATMOSPHERES

Number	$T_{eff}$	$\log \beta$	$T_{spec}/T_{eff}$	$\tau'$	$\tau_{bb}$
Hydrogen					
1.....	1.42 keV	-4	2.58	6.06	160.27
2.....		-3	2.40	6.24	63.51
3.....		-2	2.11	6.62	27.32
4.....		-1	1.79	7.22	13.01
5.....	2.84 keV	-4	2.01	4.93	173.84
6.....		-3	1.96	4.96	67.15
7.....		-2	1.83	5.06	27.83
8.....		-1	1.74	5.25	12.51
Helium					
9.....	1.42 keV	-4	2.53	6.11	107.15
10.....		-3	2.31	6.38	43.86
11.....		-2	1.96	6.86	19.78
12.....		-1	1.75	7.42	10.14
13.....	2.84 keV	-4	1.96	4.94	115.10
14.....		-3	1.91	4.99	45.72
15.....		-2	1.79	5.12	19.74
16.....		-1	1.67	5.36	9.45
Nickel					
17.....	1.42 keV	-4	2.30	6.48	34.41
18.....		-3	1.96	7.03	16.15
19.....		-2	1.67	7.50	8.96
20.....	2.84 keV	-4	1.89	5.03	35.47
21.....		-3	1.71	5.17	15.85
22.....		-2	1.59	5.42	8.14

that as the radiative flux becomes closer to the local critical flux, the density scale height in the atmosphere becomes comparable to the neutron star radius (see eq. [8] in this paper). As soon as this happens, the sphericity of the model becomes important, and the redshift variations with radius becomes as important as the variation of opacity with photon energy. All these effects must be included in the model before a meaningful comparison with observations can be made.

In spite of all the shortcomings, the model atmospheres of near-Eddington limit X-ray bursters presented in this paper are the most simple models possible that incorporate most of

the relevant physics associated with radiative transfer through a predominantly electron scattering atmosphere. Therefore, it was indeed gratifying to discover that these simple models produced results that were in remarkable agreement with results generated by much more sophisticated computer simulations.

It is our pleasure to acknowledge R. A. London for his most helpful comments. This project was partly supported by the NSF grant AST-8317116, and A. B. is supported by a NSERC (Canada) postgraduate scholarship.

## REFERENCES

- Czerny, M., and Sztajno, M. 1983, *Acta. Astr.*, **33**, 213.  
 Ebisuzaki, T., and Nomoto, K. 1985, MPA preprint No. 191.  
 Felton, J. E., and Rees, M. J. 1972, *Astr. Ap.*, **17**, 226.  
 Foster, A. J., Ross, R. R., and Fabian, A. C., 1986, *M.N.R.A.S.*, **221**, 409.  
 Fu, A. J., and Arnett, W. D., 1986, preprint.  
 Joss, P. C., and Rappaport, S. A. 1984, *Ann. Rev. Astr. Ap.*, **22**, 537.  
 Kompaneets, A. S. 1957, *Soviet Phys.—JETP*, **4**, 730.  
 Kourganoff, V. 1963, *Basic Methods in Transfer Problems* (New York: Dover).  
 Lapidus, I. I., Sunyaev, R. A., and Titarchuk, L. G. 1986, preprint.  
 Lightman, A. P. 1981, *Ap. J.*, **244**, 392.  
 London, R. A., Taam, R. E., and Howard, W. M. 1984, *Ap. J. (Letters)*, **287**, L27.  
 London, R. A., *et al.* 1986, *Ap. J.*, **306**, 170.  
 Madej, J. 1986, preprint.  
 Paczyński, B., and Anderson, N. 1986, *Ap. J.*, **302**, 1.  
 Pozdnyakov, L. A., Sobol', I. M., and Sunyaev, R. A. 1983, *Soviet Sci. Rev.*, **2E**, 189.  
 Rybicki, G. B., and Lightman, A. P. 1979, *Radiative Processes in Astrophysics* (New York: Wiley).  
 Sunyaev, R. A., and Titarchuk, L. G. 1980, *Astr. Ap.*, **86**, 121.  
 Taam, R. E. 1985, *Ann. Rev. Nucl. Part. Sci.*, **35**, 1.  
 van Paradijs, J. 1982, *Astr. Ap.*, **107**, 51.

ARIF BABUL and BOHDAN PACZYŃSKI: Princeton University Observatory, Princeton, NJ 08544